X-Band Energy Harvester with miniaturized on-chip Slot Antenna Implemented in 0.18-µm RF CMOS

Praharshin M. Senadeera, James Griggs, Zhijian Xie, and Numan S. Dogan
Department of Electrical and Computer Engineering
North Carolina Agricultural & Technical State University
Greensboro, NC, USA
pmelaka@gmail.com,{zxie,dogan}@ncat.edu

Meng Li, and Nader Behdad
Department of Electrical and Computer Engineering
University of Wisconsin
Madison, WI, U.S.A

Huseyin S. Savci
Department of Computer Engineering
Istanbul Sabahattin Zaim University
Istanbul, TURKEY

Abstract— **This paper presents a novel fully integrated X-band energy harvester, with on-chip antenna, matching network, and a multi-stage RF-DC rectifier implemented in IBM 0.18-µm RF CMOS technology. We investigated different matching schemes, antennas, and rectifiers with focus on the interaction between building blocks. Among different matching topologies, the series inductive scheme demonstrated the best performance for X-band to DC energy conversion. Our measurement results show that the proposed X-band RF-DC rectifier generates a 1.23 V DC output with 304 KΩ load at 9.2 GHz with -8.0 dBm input RF power, providing a power conversion efficiency of 3.1%.**

Keywords- Insects tracking, On-chip Slot Antennas, RF CMOS, Radio Frequency Identification (RFID), RF-DC rectifier, X-band.

I. INTRODUCTION

Radio-Frequency identification (RFID) has a wide range of applications in areas such as automated data management, tracking of desired objects, manufacturing process, and highway toll collection [1-3]. Further expansion of applications requires ultra-low cost and smaller size fully integrated passive RFID tags. The size is determined by the external battery and the antenna. In these tags the energy harvesting unit along with small antenna size is the key enabling factor [4-5].

The cost of the RFID tag can be lowered by implementing an on-chip antenna [6]. The integration of the antenna with the RFID tag allows to achieve a fully integrated single-chip wireless system with reduced cost and form factor. Low radiation efficiency is the main problem of on-chip antennas [7]. A shift to higher frequencies facilitates further miniaturization of the transponder antenna [6-7]. The lower price and miniaturization of the antenna allow new RFID applications such as tracking of insects and small objects. These tiny tags can be attached to moving insects such as honey bees, butterflies, and ants to track their movements and habitats.

Typical long range RFID applications operate below 1 GHz, where off-chip antenna is used. The shorter wavelength makes on-chip antenna a viable solution by extending the frequency to X-band. In this paper, we explore the performance of X-band CMOS RF-DC rectifier with on-chip antenna in various input matching schemes. The antenna used in this work has a much higher gain and efficiency compared to state-of-the-art on-chip antennas operating in a similar frequency range [7]. To the best of our knowledge, this is the first reported X-band CMOS RF-DC energy harvester implemented in a commercially available RF CMOS technology.

II. SYSTEM DESIGN AND CIRCUIT ANALYSIS

A. Rectifier circuit

A multi-stage rectifier circuit was used to convert input RF power to DC power (Fig. 1). Each unit cell consisted of two diode-connected NMOS transistors in series to transfer charges from the capacitor of the previous cell except for the first cell. Both coupling and storage capacitors along with parasitics play critical roles in the rectifier X-band performance. The ZVT (zero-threshold) NMOS transistors are used to maximize rectifier performance [2]. Using the charge conservation principle, we derived the final DC output voltage as,

$$V_{out} = 2N\left(V_{rf} - V_{th}\right) - \frac{I_{out}}{f}\left(\sum_{k=1}^{N}\frac{1}{Co_k} + \sum_{k=1}^{N}\frac{1}{CL_k}\right) \quad (1)$$

where V_{out} is the DC output voltage and I_{out} is the DC output current, N is the number of cells in RF rectifier, V_{rf} is the input RF amplitude at the coupling capacitor terminal, V_{th} is the threshold voltage of ZVT (actually ~22mV).

We then define C_{eff} as,

$$\frac{1}{C_{eff}} = \sum_{k=1}^{N}\frac{1}{CO_k} + \sum_{k=1}^{N}\frac{1}{CL_k} \quad (2)$$

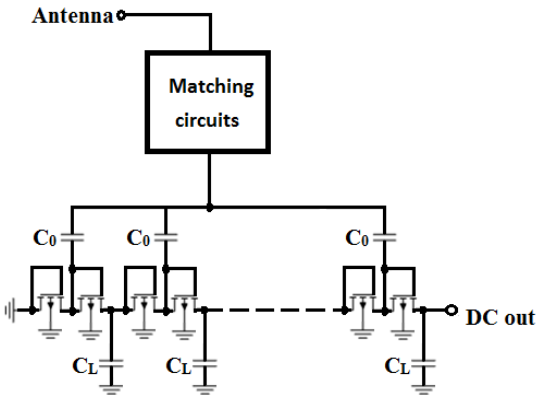

Fig. 1. Schematic of energy harvester for passive RFID transponder.

V_{out} is expressed as,

$$V_{out} = 2N\left(V_{rf} - V_{th}\right) - \frac{I_{out}}{f.C_{eff}} = V_{oc} - I_{out}R_{out} \quad (3)$$

where

$$V_{oc} = 2N(V_{rf} - V_{th}),\ R_{out} = \frac{1}{f.C_{eff}} \quad (4)$$

V_{oc} is the open-circuit voltage and R_{out} is the internal resistance of the rectifier.

Essentially, C_{eff} is equivalent to the series connection of all load capacitors and coupling capacitors in the rectifier units. The parasitic capacitances of transistors were omitted in this analysis. In practice, they can be considered to be absorbed into coupling and storage capacitors. Contrary to the conventional design rule of thumb where C_o needs to be much larger than C_L, the above analysis shows that C_o and C_L contribute equally to C_{eff}. They also contribute equally to the input impedance of the rectifier block. As we can see, when I_{out} is zero, (3) becomes the same as the first order estimation. The output resistance of the DC source is given by $1/(f\ C_{eff})$. This provides guidance in choosing coupling and load capacitances.

The size of all the diode-connected transistors is alsoconstrained by their parasitic capacitances, i.e. wide transistors provide large charging current for capacitors but require more charges to turn them on or off. Transistor sizes also contribute to the overall admittance and directly impact the matching network design.

B. *Matching Network*

Due to the nonlinear nature of the rectifier, the matching network design differs from the one for a linear RF system. Voltage boosting was emphasized because the Zero-VT transistors require a non-zero voltage (~22 mV) to turn on.

Many different matching networks were considered and simulated. The cases shown in Figs. 2(a) and 2(b) are among the most promising solutions, while that in Fig. 2(c) is no-matching case (direct feed into the rectifier). All three cases were extensively optimized and implemented in the final layout.

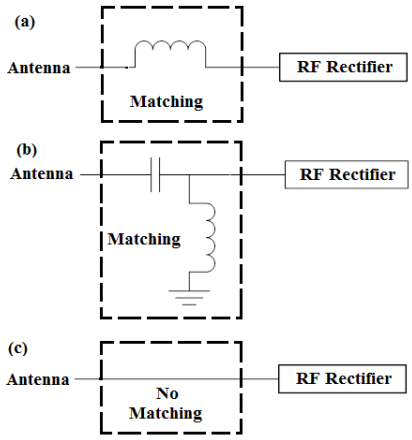

Fig. 2. Matching network for multistage rectifier, (a) series inductor matching; (b) series capacitor-shunt inductor matching; (c) direct feed through without matching.

Table I and II present the values of the circuit components, transistor sizes, and simulated rectifier performance of the X-Band CMOS rectifier with series inductor matching and parallel inductor/series capacitor matching.

TABLE I. DESIGN VALUES

Technology	IBM 0.18µm RF CMOS
Number of Rectifier stages	6
Coupling capacitors	MIM Cap, C_{eff} =150fF
Load capacitors	MIM Cap, C_{eff} =150fF
Transistors	ZVT W/L=3µm/0.7µm
Operating Frequency	~10GHz
RF amplitude	300mV

TABLE II. SIMULATED PERFORMANCE OF TWO CASES

	Series Inductor	**Parallel Inductor Series Capacitor**
Layout area	200µm x 150µm	100µm x 150µm
Matching elements	L_S=2.76nH	L_P=1.37nH C_S=128.17fF
Vout @250KΩ	1.76V@ -8.1dBm	1.32V@ -8.1dBm
Conv. Eff. @250KΩ	8% @ -8.1dBm	3.09%@ -8.1dBm
Equiv. Rs	~100KΩ	~100KΩ

The rectifier circuit was simulated by both AC and transient analysis. Transistors were ZVT NMOS with gate length of 700 nm. We compared rectifiers with 3 to 10 stages. With the increased number of stages, matching became more difficult. Our analysis revealed that about 6 stages provide the best performance. When the rectifier has more than 6 stages, increased transistor parasitic losses reduced the total rectified voltage.

C. *Antenna*

Slot antenna was designed according to the principle given in [7]. They can be considered to be dual of dipole- or wire-type antennas. With the high metallization density, slot

antenna minimizes the conductive loss in its metal layer. This is particularly important for miniaturized antennas, since their radiation resistances are usually very small. Therefore, by using a miniaturized slot topology, the radiation efficiency of small on-chip antennas can be enhanced. The antenna covers an area of 0.55mm^2.

III. Experimental Results And Discussion

The energy harvester and its building blocks were successfully fabricated in 0.18-µm CMOS process. The fabricated circuit building blocks include; (i) 6-stage RF-DC rectifier, (ii) 6-stage RF-DC rectifier with different matching circuits, (iii) slot antenna, and (iv) Integrated 6-stage RF-DC rectifier with slot antenna.

A. Rectifier with and without matching circuits

Fig. 3 shows the layout of the RF-DC rectifier with series inductive matching and the probe setup for measurement. The RF signal was generated by Agilent 8341A vector signal generator.

Fig. 4 shows the output voltage of the RF-DC rectifier as a function of input RF frequency. The rectifier with series inductor matching shows the highest output voltage in the frequency range from 9.0 GHz to 9.6 GHz. The rectifier with parallel inductor and series capacitor matching also shows conversion peak at about 9.5 GHz, but with significantly lower output voltage. Meanwhile, the rectifier without any matching produces significantly lower output voltage in the X band as expected.

Fig. 5 shows the dependence of DC output voltage on load impedance. The extracted equivalent internal source resistance at P_{in} = -10 dBm is 85.8 KΩ, which is close to the value extracted from simulation results (100 KΩ). Compared with Cadence Spectre simulation result, the measurement data shows lower optimum frequency, 9.0~9.6 GHz versus 10 GHz in simulation and lower DC output, which is largely attributed to the circuit parasitics.

Fig. 6 shows the DC voltage generated by the power harvester circuit for different levels of the input signal power at 9.2 GHz. The circuit exhibits 3.1% power conversion efficiency for -8 dBm input power.

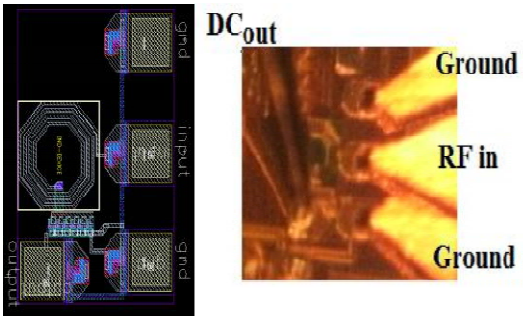

Fig. 3. Layout and probing setup of series inductive matched RF-DC Rectifier.

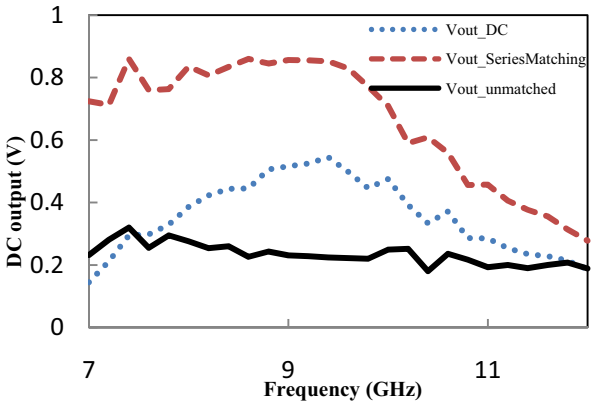

Fig. 4. Rectifier output voltage versus RF frequency for -10 dBm input power and 304 KΩ load impedance.

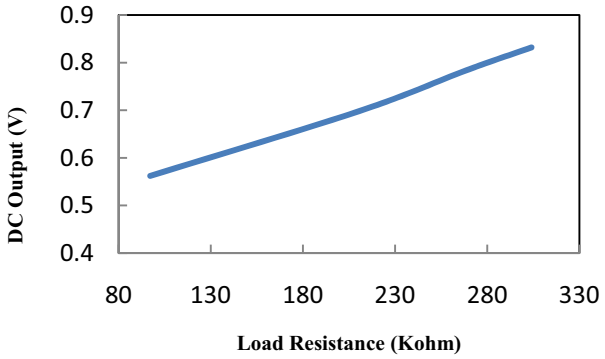

Fig. 5. DC output voltage with different load resistance, RF input at 9.2 GHz and power of -10 dBm.

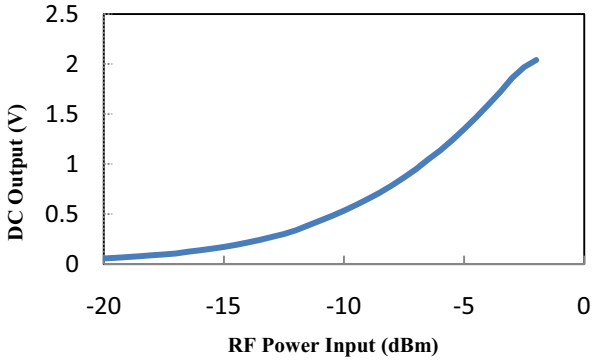

Fig. 6. DC output voltage versus RF input power at 9.2 GHz with load impedance of 304 KΩ.

B. Antenna

Fig. 7 shows the fully integrated RF-DC rectifier with miniaturized slot antenna. We used the rectifier with series inductive matching since it produced the highest DC output voltage to integrate with the slot antenna. To characterize the antenna itself, separate antenna with GSG pad was also included in the final layout. The measurement setups for both structures are shown in Figs. 8 (a) and 8(b).

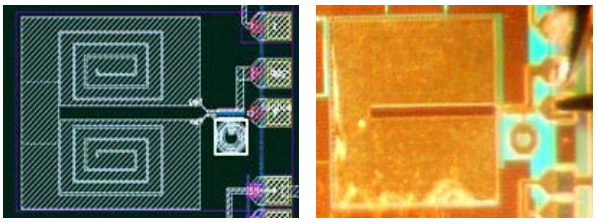

Fig. 7. Layout and microphotograph of the RF-DC Rectifier with slot antenna.

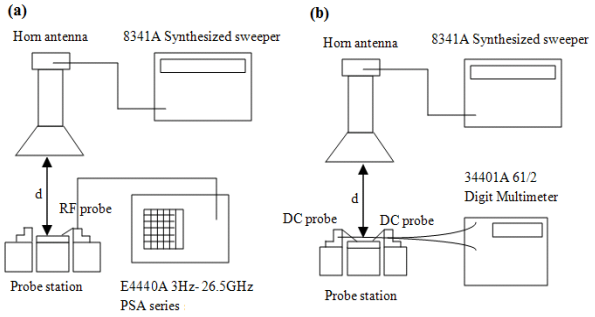

Fig. 8. (a) on-chip probing setup used to measure slot antenna; (b) on-chip measurement setup used to measure the rectified voltage of the RF-DC rectifier with slot antenna.

The RFOUT of the Agilent 8341A vector signal generator was connected to the WR-90 horn antenna which has the frequency band of 8.2 GHz to 12.4 GHz and nominal gain of 15 dB. The electromagnetic waves from the horn antenna were received by the slot antenna.

To measure the received power spectrum, the antenna was probed directly by Cascade Microtech GSG probe connected to the E4440A (3 Hz – 26.5 GHz) series spectrum analyzer. Fig. 9 shows the received power versus antenna range for 10 dBm source power at 10 GHz.

The power arrived at the slot antenna, P_r, can be calculated using the Friss free-space equation. The Friss free-space equation in dBm is as follows:

$$P_r = P_t + G_t + G_r - 20log_{10}\left(\frac{4\pi d}{\lambda}\right) \quad (5)$$

where, P_t is the power transmitted by the transmitting antenna, G_t is the gain of the transmitting antenna, G_r is the gain of the receiving antenna, λ is the wavelength, and d is the distance between the receiving and transmitting antenna.

Fig.10 shows the slot antenna gain versus the distance calculated from the Friss equation (5) and data in Fig. 9. The best gain of the slot antenna was achieved when the distance between the two antennas was from 24 cm to 60 cm.

Our model uses the following parameters: For a one data set

- d = 0.24 m
- λ = 0.03 m (f = 10 GHz)
- P_t = 10 dBm (8341 synthesized sweeper power)
- G_t = 15 dB (WR-90 horn antenna 8.2 – 12.4 GHz power)
- P_r = -37.05 dBm (Received power of EM4440A spectrum analyzer)

From (5) => G_r = -22.0 dB. With all the data points the receiver antenna gain (G_r) can be obtained as -22 dB.

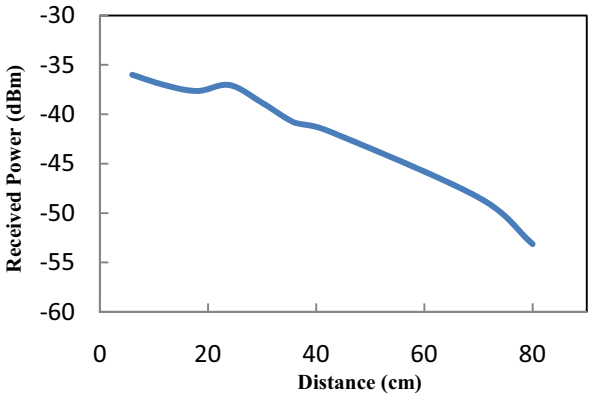

Fig. 9. Power received by slot antenna versus the distance between antennas with source power of 10 dBm.

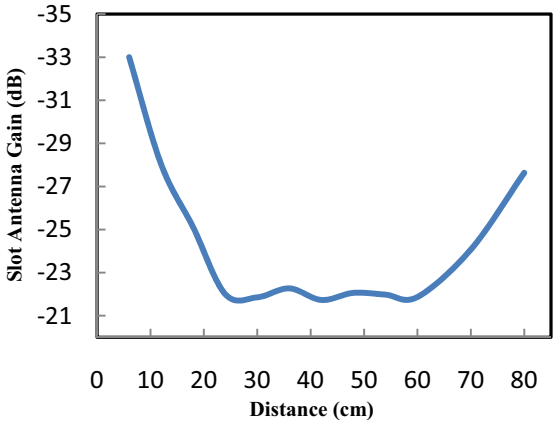

Fig. 10. Receiver antenna gain versus the distance between antennas with source power of 10 dBm.

Fig.11 shows the DC voltage generated by the power harvester for different levels of source power. In this figure power harvester circuit generates a maximum DC output in the frequency band of 9-10 GHz. These test results are in very good agreement with the simulation results.

C. RF-DC rectifier with integrated antenna

The fully integrated energy harvester was implemented as a 6 stage RF-DC rectifier connected to the slot antenna. Fig.12 shows the generated DC output of the X-band energy harvester with different levels of source power. When the source power increased from 0 dBm to 10 dBm the DC output increase gradually from 0 mV to 40 mV. When the source power was increased beyond 10 dBm there was a rapid increase of the DC output from 40 mV to 100 mV.

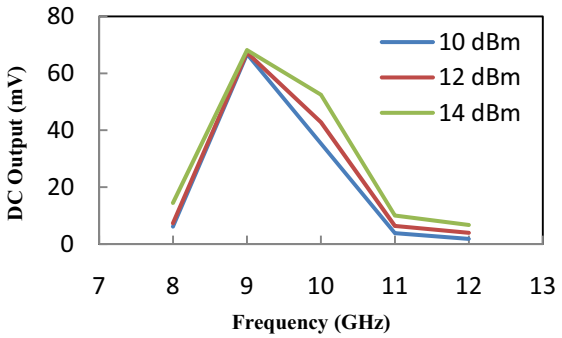

Fig. 11. DC output voltage versus input signal power at 10 GHz at the antenna range of 6cm.

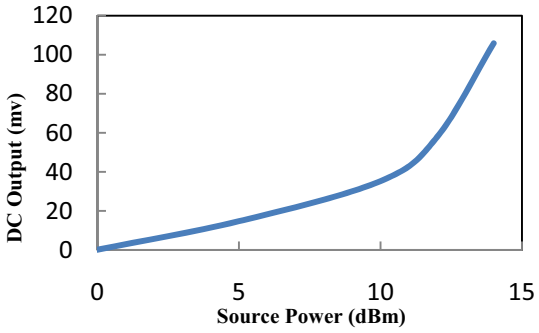

Fig. 12. DC output voltage versus input signal power at 10 GHz at the antenna range of 6cm

IV. Conclusion

We implemented a novel fully integrated X-band energy harvester in IBM 0.18-µm RF CMOS technology with on-chip antenna which is smaller than the previously reported antennas. The novel on-chip miniaturized slot antenna occupies less space compared to the traditional off-chip antennas. The proposed antenna covers an area of 0.55mm^2. The smaller size and the cost of the RFID tag are critical for widespread adoption of the technology. The cost of the RFID tag can be lowered by implementing an on-chip antenna.

The lower price and miniaturization of the antenna allow new RFID technology applications such as insects tracking. These tiny tags can be attached to moving insects such as honey bees, butterflies, and ants to track their movements and habitats. The other key design issues addressed in this paper include the roles of coupling and load capacitors in a multistage rectifier, different matching networks for voltage boosting and efficient power transfer from a source.

Our simulation and measurement results show that the single series inductor provides the best matching for the multi-stage rectifier. The matched rectifier generated 1.23V DC output voltage with 304 KΩ load at 9.2 GHz for -8 dBm direct X-band input through the GSG probe. Our results show the feasibility of a fully integrated passive RFID transponder with on-chip antenna in X-band frequency.

References

[1] S. Han, H Lim, J. Lee, "An efficient localization scheme for a differential-driving mobile robot based on RFID system," IEEE Transactions on Industrial Electronics, vol. 54, pp. 3362–3369, 2007.

[2] Y. Yao, M Tasi, S. Hsu, F. Hsueh, C. Jou, M. Song, J. Tseng, T. Chang, D, Nag, "A Fully Integrated 900-MHz Passive RFID Transponder Front End With Novel Zero- Threshold RF–DC Rectifier," *IEEE Transactions on Industrial Electronics*, vol. 56, pp. 2317–2325, 2009.

[3] Q. Huang and M. Oberle, "A 0.5-mW passive telemetry IC for biomedical applications," *IEEE Journal of Solid- State Circuits*, vol. 33, pp. 937–946, 1998.

[4] F. Mazzilli, P.E. Thoppay, N. Johl, C. Dehollain, "Design methodology and comparison of rectifiers for UHF-band RFIDs," *IEEE Radio Frequency Integrated Circuits* (RFIC) Symphosium, Anaheim, CA, pp. 505–508, 2010.

[5] S. Mandal and R. Sarpeshkar, "Low-power CMOS rectifier design for RFID applications," *IEEE Transactions on Circuits and Systems* I: Regular Papers, vol. 54, pp. 1177–1188, 2007.

[6] L.Vojtech, "RFID Transponder in X-Band and its Feasibility," *Second International Conference on Sensor Technologies and Applications-Sensorcomm*, Cap Esterel, France, pp. 99–102, 2008.

[7] N. Behdad, D. Shi, W. Hong, K. Sarabandi, and M.P. Flynn, "A 0.3 mm2 Miniaturized X-Band On-Chip Slot Antenna in 0.13µm CMOS," *IEEE Radio Frequency Integrated Circuits Symposium*, pp. 441–444, 2007.